SCIENCE CHINA
Life Sciences

• RESEARCH PAPERS •

October 2010 Vol.53 No.10: 1196–1203
doi: 10.1007/s11427-010-4075-4

Cell-death-mode switch from necrosis to apoptosis in hydrogen peroxide treated macrophages

LIN XuZhu, SUN TingZhe, CAI MeiHong & SHEN PingPing*

State Key Laboratory of Pharmaceutical Biotechnology, Department of Biochemistry, School of Life Science, Nanjing University, Nanjing 210093, China

Received November 29, 2009; accepted December 6, 2009

Cell death is typically defined either as apoptosis or necrosis. Because the consequences of apoptosis and necrosis are quite different for an entire organism, the investigation of the cell-death-mode switch has considerable clinical significance. The existence of a necrosis-to-apoptosis switch induced by hydrogen peroxide in macrophage cell line RAW 264.7 cells was confirmed by using flow cytometry and fluorescence microscopy. With the help of computational simulations, this study predicted that negative feedbacks between NF-κB and MAPKs are implicated in converting necrosis into apoptosis in macrophages exposed to hydrogen peroxide, which has significant implications.

macrophage, hydrogen peroxide, apoptosis, necrosis, cell-death-mode switch

Citation: Lin X Z, Sun T Z, Cai M H, *et al*. Cell-death-mode switch from necrosis to apoptosis in hydrogen peroxide treated macrophages. Sci China Life Sci, 2010, 53: 1196−1203, doi: 10.1007/s11427-010-4075-4

In the last decade, increasing attention has been focused on the mechanism underlying the cell-death-mode switch [1]. Cell death is typically defined dichotomously as either apoptosis or necrosis. Apoptosis is considered to be superior to necrosis in that the former is not accompanied by local and general reactions because apoptotic cells are phagocytized by neighboring cells. By contrast, necrosis, especially when it occurs massively, often results in serious inflammation, organ failure or mortality [2]. Hence, the disparity between apoptosis and necrosis is critical especially for clinical medicine. Though the switch mechanism has been studied in diverse cell types [3–5], seldom has it been reported in immune cells.

Macrophages are a pivotal factor in the innate immune system through recognizing and destroying altered host compounds and invading microorganisms. Although they survive for a relatively long time in a physiological condition, their demise caused by such stimuli as cytokines, bacterial invasion, or ER stress is frequently observed in pathological conditions [6–8]. One of these stimuli is excessive ROS (reactive oxygen species, including superoxide, peroxide and free radicals) [9,10]. Thus, there is considerable clinical significance in studying macrophage cell death caused by ROS.

Besides the induction of cell death, ROS also elicits several pathways in macrophages, involving the MAPKs (mitogen-activated protein kinases) pathway and the NF-κB (nuclear factor-κB) pathway [11,12]. MAPKs include three subfamilies, the best characterized of which are ERK (extracellular regulated proteinkinase), JNK (Jun N-terminal kinase) and p38-MAPK. NF-κB is normally retained in the cytoplasm by its inhibitory protein I-κB. Once I-κB is phosphorylated and degraded, NF-κB is activated and translocated into the nucleus. Though both MAPKs and NF-κB pathways are reported to be closely related to cell death [13,14], investigations about their functions in the cell-death-mode switch are underdetermined.

*Corresponding author (email: ppshen@nju.edu.cn)

The purpose of the present study was to analyze the cell-death-mode switch in RAW 264.7 cells (a murine macrophage cell line) subjected to hydrogen peroxide. We firstly demonstrated that a necrosis-to-apoptosis switch did occur, based on flow cytometric and immunofluorescent evidence. We detected the alterations of MAPKs and NF-κB during a time course. Through introducing two mathematical models, we proposed a possible explanation how MAPKs and NF-κB worked together to regulate this necrosis-to-apoptosis switch. This switch may benefit the organisms confronted with pathogens by shielding them from serious inflammation.

1 Materials and methods

1.1 Reagents and antibodies

Hydrogen peroxide was dissolved in water and stored in 10 mol L^{-1} which was freshly diluted with a culture medium to the indicated concentrations before use. The DMEM medium was obtained from Hyclone (Logan, UT). Fetal bovine serum was purchased from PAA Laboratories (Pasching, Austria). All antibodies were obtained from Cell Signaling Technology (Beverly, MA). All chemicals were obtained from Sigma Chemicals (St. Louis, MO) unless otherwise stated. All kits were bought from Beyotime Institute of Biotechnology (Jiangsu, China).

1.2 Cell culture

A RAW 264.7 macrophage cell line was obtained from the Shanghai Institutes for Biological Sciences. The cells were maintained in a DMEM medium supplemented with 10% fetal bovine serum, 2 mmol L^{-1} L-glutamine and 100 μg mL^{-1} gentamycin in a humidified atmosphere of 5% CO_2 at 37°C. All experiments were performed using a DMEM medium with the same supplementation except that fetal bovine serum was at 1%.

1.3 Annexin V-PI staining

ROS-induced cell death was determined by an annexin V–PI kit according to the manufacturer's instructions. Macrophages incubated with H_2O_2 were harvested and twice washed with cold phosphatebuffered saline (PBS). Cells were resuspended in a binding buffer at a concentration of 1×10^6 cells mL^{-1} and 200 μL cell suspension was subsequently transferred to a 5-mL culture tube, treated with 5 μL annexin V and 10 μL propidium iodide (PI) at 37°C for 15 min in the dark. The cells were subsequently diluted with 200 μL of binding buffer and 10000 cells in each group were analyzed on a FACS Calibur (Becton Dickinson, USA) equipped with a single laser emitting excitation light at 488 nm.

1.4 Immunofluorescence study

Cells treated with H_2O_2 for either 3, 5 or 7 h were washed in PBS and stained with Hoechst 33342 (final concentration 5 μmol L^{-1}) and PI (final concentration 0.5 μmol L^{-1}) in the dark for 10 min at 37°C. Cells were washed twice with PBS and fixed with 2% paraformaldehyde for 10 min. Fields of cells were photographed, by using appropriate filters to examine the Hoechst 33342 and PI fluorescence staining.

1.5 Western blotting

After being incubated with hydrogen peroxide, cells were harvested and suspended in 300 μL lysis buffer (50 mmol L^{-1} Tris-HCl (pH 8.0), 150 mmol L^{-1} NaCl, 1 mmol L^{-1} EDTA, 10% glycerol, 1 mmol L^{-1} DTT, 1% NP-40, 1 mmol L^{-1} PMSF) at 4°C for 30 min. Cell debris was removed by centrifugation at 12000×*g* for 10 min at 4°C, and the supernatants were collected and stored at −70°C until use. Protein concentration of cell lysate was determined utilizing the Bradford method. The proteins (50 μg per sample) were electrophoresed on 8%, 10%, 12% or 15% sodium dodecyl sulfate polyacrylamide gels (SDS-PAGE), before being electrotransferred onto a polyvinylidene fluoride (PVDF) membrane (Amersham, UK). After being blocked in PBS containing 0.1% Tween 20 with 5% skimmed milk powder at 37°C for 4 h, the membrane was incubated overnight with primary antibody. The detection step was performed with horseradish peroxidase (HRP)-conjugated antibody. The target proteins were visualized with an Enhanced Chemiluminescent Method kit (SABC, China).

1.6 Preparation of crude nuclear extracts and electrophoretic mobility shift assay (EMSA)

Cells pro-treated with hydrogen peroxide were harvested and suspended in 400 μL buffer A (10 mmol L^{-1} Hepes, 10 mmol L^{-1} KCl, 0.1 mmol L^{-1} EDTA, 0.2% NP-40, 1 mmol L^{-1} DTT, 0.1 mmol L^{-1} PMSF, 1 mg L^{-1} leupeptin, antipain, aprotinin and pepstatin) at 4°C for 10 min. With 25 μL 10% NP-40 interfused for 15 s, cell debris was collected by centrifugation at 12000×*g* for 5 min at 4°C. The deposition was resuspended in 60 μL buffer B (20 mmol L^{-1} Hepes, 420 mmol L^{-1} NaCl, 0.1 mmol L^{-1} EDTA, 1.5 mmol L^{-1} MgCl, 25% glycerol, 1 mmol L^{-1} DTT, 0.1 mmol L^{-1} PMSF, 1 mg L^{-1} leupeptin, antipain, aprotinin and pepstatin) at 4°C for 20 min. After centrifugation at 12000×*g* for 10 min at 4°C, the supernatants were collected and stored at −70°C until use.

A double-stranded oligonucleotide containing NF-κB motif (5′-GAAGCATGGGGACTCTCC-3′ and 5′-TTCCC-AAAGGGAGAGTCCCCAAGCTTC-3′) was labeled with [γ-^{32}P] ATP by the kinase reaction. Approximately 0.1 pmol of the labeled probe was incubated with 5 μg of nuclear

extract in a reaction mixture (10 mmol L^{-1} HEPES-KOH, pH 7.9, 50 mmol L^{-1} KCl, 2.5 mmol L^{-1} $MgCl_2$, 1 mmol L^{-1} dithiothreitol, 10% glycerol, and 2 μg of poly-I:C). After 15–30 min of incubation at room temperature, the DNA-protein complexes were fractionated on a 6% non-denaturing polyacrylamide gel in 0.5×TBE at room temperature. The specificity of the binding reaction was confirmed by a competition assay with a 100-fold molar excess of unlabelled probe.

1.7 Mathematical modeling

We adopted two simple models to investigate the connections between MAPKs (M) and NF-κB (N) as well as their roles in the necrosis-to-apoptosis switch. Only the activation and deactivation rates are considered in the equations for simplicity (Table 1). A Hill function, which indicates a nonlinear inhibitory effect (NF-κB dependent inhibition of MAPK activation), is represented as $G_i(N)$. Delays are also discussed in our equations. The DDEs (delayed differential equations) were numerically integrated by a Matlab (Mathwork, R2006b, release 14) dde23 operator.

Table 1 Parameter details of mathematical models

Parameter	Description	Value
a_m	MAPK activation rate	0.01
σ_m	MAPK deactivation rate	0.3
a_n	NF-κB activation rate	0.1
σ_n	NF-κB deactivation rate	0.015
E_0	Normalized regression threshold	0.05
n	Hill coefficient	5
τ_m	MAPK time delay	80
k_1	Coefficient for p38 mediated apoptosis activation	0.001
k_2	p38 mediated transformation from necrosis to apoptosis	0.05
k_3	JNK mediated transformation from apoptosis to necrosis apoptosis repression	0.005
k_4	Coefficient for ERK mediated apoptosis repression	0.05
k_5	Coefficient for JNK mediated apoptosis activation	0.1
k_6	Coefficient for JNK mediated necrosis activation	0.06
k_7	Coefficient for ERK mediated necrosis repression	0.001
I_A	NF-κB mediated apoptosis repression	0.001
I_N	NF-κB mediated necrosis repression	0.001

$$dM_1/dt = a_m \cdot G_1(N) - \sigma_m \cdot M_1, \quad (1)$$

$$dN/dt = a_n \cdot M(t-\tau_m) - \sigma_n \cdot N, \quad (2)$$

$$dM_2/dt = a_m \cdot G_2(N) - \sigma_m \cdot M_2, \quad (3)$$

$$dM_3/dt = a_m \cdot G_3(N) - \sigma_m \cdot M_3, \quad (4)$$

$$\begin{aligned} dA_{frac}/dt = {} & k_1 \cdot M_1 \cdot (1 - A_{frac} - N_{frac}) \\ & + k_2 \cdot M_1 \cdot N_{frac} - k_3 \cdot M_3 \cdot A_{frac} \\ & - k_4 \cdot M_2 + k_5 \cdot M_3 \cdot (1 - A_{frac} - N_{frac}) \\ & - I_A \cdot N \cdot A_{frac}, \end{aligned} \quad (5)$$

$$\begin{aligned} dN_{frac}/dt = {} & k_6 \cdot M_3 \cdot (1 - A_{frac} - N_{frac}) \\ & + k_3 \cdot M_3 \cdot A_{frac} - k_2 \cdot M_1 \cdot N_{frac} \\ & - k_7 \cdot M_2 - I_N \cdot N \cdot N_{frac}, \end{aligned} \quad (6)$$

where $G_i(N) = \dfrac{1}{1 + [\dfrac{N(t-\tau_i)}{E_0}]^n}$ (i=1, 2 and 3).

A_{frac} and N_{frac} respectively donate apoptotic and necrotic fractions of cells, while $1-A_{frac}-N_{frac}$ represents fractions of normal cells. M1, M2 and M3 respectively represent the phosphorylated form of p38, ERK and JNK.

1.8 Statistical analysis

Data was expressed as the mean±standard error (SE). Statistical analysis was performed by students' *t*-test. $P<0.05$ or $P<0.01$ was considered statistically significant and indicated by ∗ or ∗∗, respectively.

2 Results

2.1 A necrosis-to-apoptosis switch occurred in macrophages exposed to H_2O_2 after a period of treatment

To verify hydrogen peroxide-induced cell death, RAW 264.7 macrophage cells were exposed to increasing doses of hydrogen peroxide of 100, 200, 300, 400 and 500 μmol L^{-1}. Cell death was evaluated 4 h later by annexin V/PI double staining. As seen in Figure 1A, increasing amounts of hydrogen peroxide induced a significant dose-dependent elevation of macrophage death. Exposure to doses of either 0, 100, 200, 300, 400 or 500 μmol L^{-1} hydrogen peroxide resulted in approximate values of respectively 3.0%, 3.6%, 7.8%, 11.6%, 19.1%, 20.8% apoptotic cells and 4.9%, 5.2%, 7.9%, 7.1%, 16.5%, 23.7% necrotic cells. Time-sequential measurements of the proportions of apoptotic cells and necrotic cells were made to analyze the possible cell-death-mode switch. RAW 264.7 cells were analyzed by annexin V/PI staining after exposure to 500 μmol L^{-1} hydrogen peroxide for either 0.5, 1, 2, 4 or 6 h. At this concentration of hydrogen peroxide, a sustained and distinct increase of apoptotic cell number was observed, while the necrotic cell number progressively rose within the first 4 h of treatment before significantly dropping by 8% at 6 h, as shown in Figure 1B. The ratio of apoptotic cells to necrotic cells did not exhibit considerable variety until 4 h when it rose from around 1.0 to approximately 2.0, indicating a necrosis-to-apoptosis switch had occurred.

Therefore, we employed immunofluorescence to confirm the existence of intermediate cells undergoing the change from necrosis to apoptosis. We photographed the H_2O_2-treated cells stained with Hoechst 33342 and PI by applying appropriate filters. As shown in Figure 2B, a large number

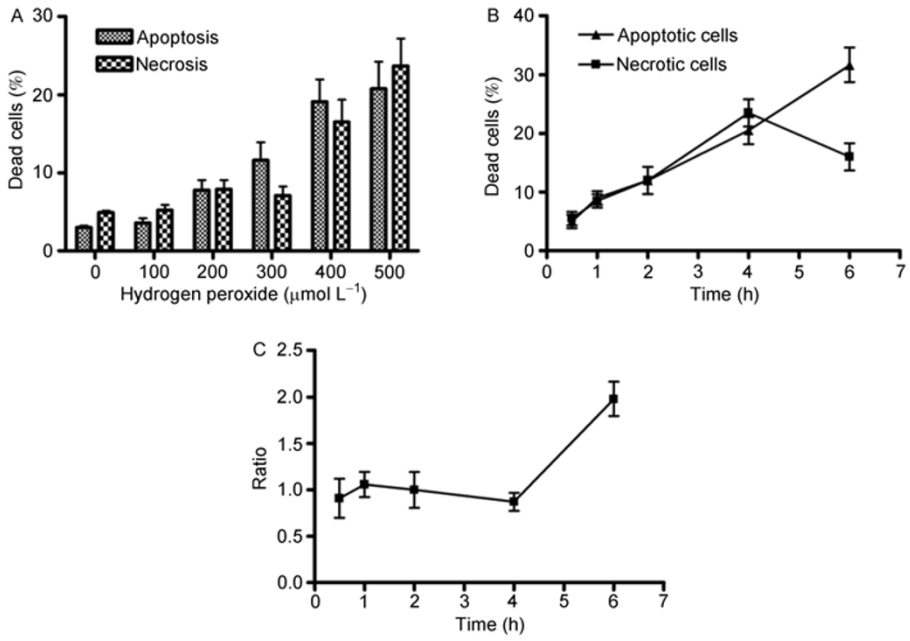

Figure 1 Necrosis-to-apoptosis switch occurred after a period time of treatment. A, Cells were exposed to 0, 100, 200, 300, 400 and 500 μmol L^{-1} hydrogen peroxide for 4 h. After treatment, cells were harvested before being stained with annexin V and PI. The percentages of necrotic cells and apoptotic cells were determined by flow cytometry. B, Cells were treated with 500 μmol L^{-1} hydrogen peroxide for either 0.5, 1, 2, 4 or 6 h. After the indicated time, cells were subjected to annexin V-PI staining. The percentages of necrotic cells and apoptotic cells were determined by flow cytometry and exhibited as ■ and ▲. C, The apoptotic cells/necrotic cells ratio within 6 h is shown. The experiment was repeated twice.

of apoptotic cells characterized by bright blue condensed nuclei mono-stained with Hoechst 33342 (green arrow) as well as necrotic cells distinguished by red normal-size nuclei mono-stained with extensive PI (white arrow) are observed when macrophages were exposed to H_2O_2 for 3 h. By comparison with Figure 2B, few typical necrotic cells are seen from the photograph of macrophages treated with H_2O_2 for 5 h (Figures 2C and E), whereas many cells whose DNA were stained by substantial PI are found not only containing shrinking nuclei but their nuclei tend to exhibit a light blue color (brown arrow). We characterized these cells as intermediate cells changing from necrosis to apoptosis. In the picture of macrophages with 7 h H_2O_2 treatment (Figure 2D), relatively few necrotic cells are visible with apoptotic cells having contracted double nuclei stained with Hoechst 33342 and PI (red arrow), which are presumed to have come from the intermediate cells. In conclusion, we have demonstrated the existence of a cell-death-mode switch from necrosis to apoptosis in hydrogen peroxide treated RAW 264.7 macrophages.

2.2 H_2O_2-induced NF-κB variation in RAW 264.7 macrophages

There have been numerous reports noting that NF-κB is associated, to a great extent, with cell death [13], so we detected the variation of NF-κB in RAW 264.7 cells exposed to 500 μmol L^{-1} hydrogen peroxide. EMSA was used to evaluate the activation of NF-κB, and the phosphorylation of I-κB was measured by Western blotting. As seen in Figure 3A, NF-κB activation did not significantly increase until 2 h post-induction, when it peaked at 4 h of treatment. After that, the activation returned to the basal level. Consistent with this phenomenon, little IκB was phosphorylated within 1 h, thereafter p-IκB significantly increased after 1 h and reached the maximum at about 2 h, before returning to a relatively low level (Figure 3B).

2.3 H_2O_2-induced MAPKs activation in RAW 264.7 macrophages

Many MAPKs including JNK, ERK and p38 are closely correlated with cell death [14], thus we analyzed ROS-induced phosphorylations of MAPKs in RAW 264.7 cells challenged with 500 μmol L^{-1} hydrogen peroxide. As shown in Figure 4, the activation of JNK was intense, reaching maximum values within 2 h after treatment, decreasing thereafter and reaching a control level at about 6 h. Similarly, the activation of ERK was also observed at 0.5 h of H_2O_2 treatment, reaching the maximal level at 2 h with a progressive decrease thereafter. We further examined p-p38. It exhibited a rapid increase and peaked at 0.5 h, thenceforth it progressively lessened to the basal level at around 2 h. Nevertheless, it returned to a high level at 4 h. In general, these alterations are likely to mediate the molecular mechanism of the cell-death-mode switch.

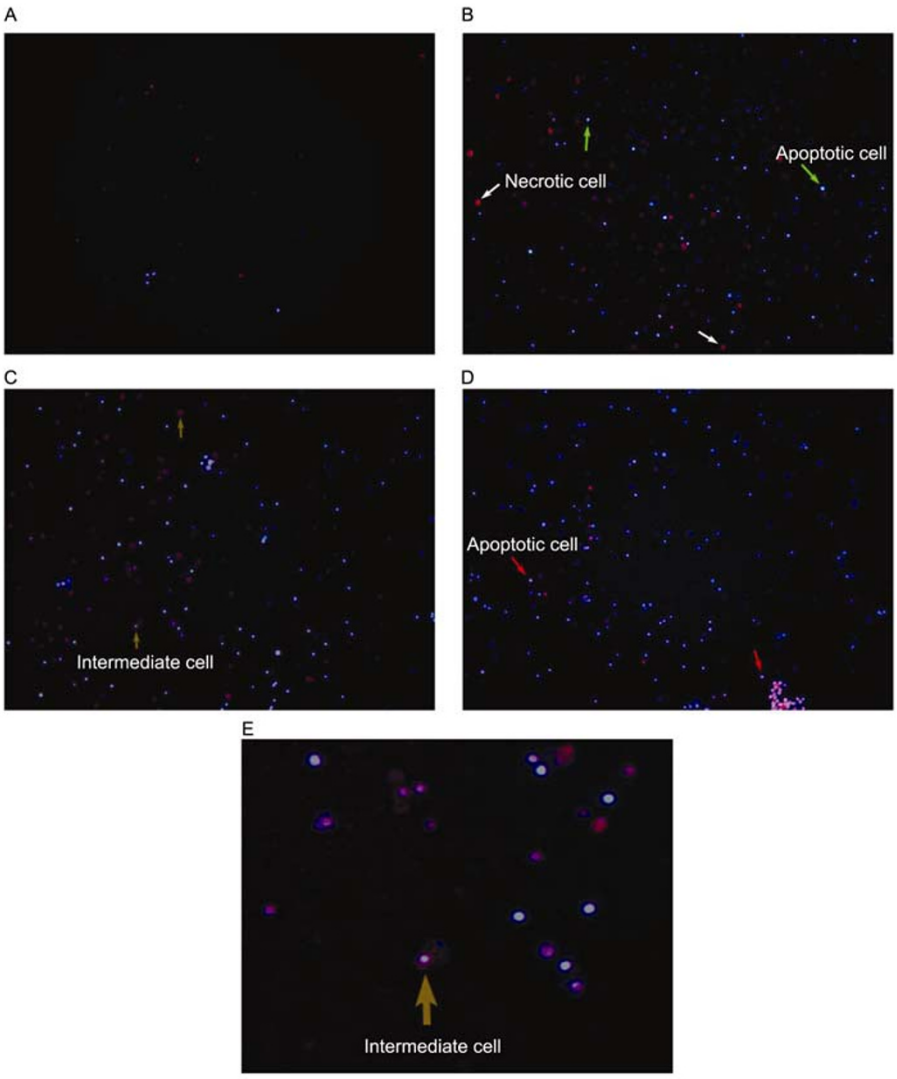

Figure 2 Intermediate cells undergoing necrosis to apoptosis were observed with fluorescence microscopy. The cells were stained with a color combination of DNA-specific dyes Hoechst 33342 (blue) and PI (red). A, Scattered dead cells are shown in the paragraph of control cells. B, Cells were treated with 500 μmol L^{-1} H_2O_2 for 3 h. Apoptotic cells are indicated by green arrows and necrotic cells are emphasized by white arrows. C, Cells were exposed to 500 μmol L^{-1} H_2O_2 for 5 h. Intermediate cells are highlighted by brown arrows. D, Cells were treated with 500 μmol L^{-1} H_2O_2 for 7 h. Apoptotic cells originating from intermediate cells are indicated by red arrows. E, The details of intermediate cells are shown. This experiment was repeated twice.

2.4 Analysis of the connections between NF-κB and MAPKs via mathematical modeling

Based on previous reports, we considered one minimal model of NF-κB and MAPKs (respectively p-p38, p-ERK, p-JNK) interactions (Figure 5A). Because the interaction network covers a plethora of components and current knowledge of the system is incomplete, we adopted a simplified two-component model to capture the characteristics of their regulations. Parameters are non-dimensional. Application of non-dimensional parameters is favorable for mathematical analysis without loss of topological characteristics.

We introduced τ_i (i=1, 2 or 3) as a time delay for NF-κB dependent repression of MAPK. Once activated by H_2O_2, MAPKs positively regulate NF-κB activity with a time delay τ_m. Activated NF-κB inhibits upstream MAPK with distinct time delays (τ_i). A small τ_i value indicates that the negative regulatory effects are fast, while large τ_i value denotes slow negative regulations.

As shown in Figure 5B, compared to Figures 3 and 4, the activation patterns of NF-κB and the three MAPKs are approximately simulated, demonstrating the reliability of this model.

2.5 Simulating a necrosis-to-apoptosis switch via mathematical modeling

Based on the above results, common recognitions and our predictions, we further introduce another model to elucidate

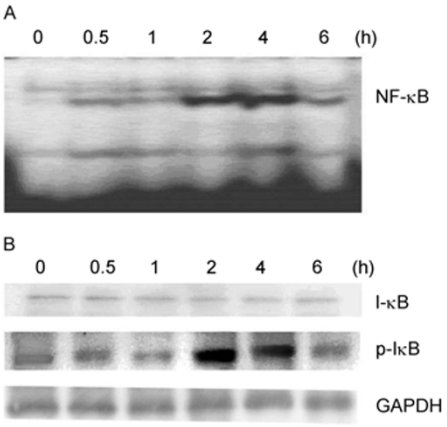

Figure 3 H_2O_2 induced the activation of NF-κB in RAW 264.7 macrophages. Cells were treated with 500 μmol L^{-1} hydrogen peroxide for either 0.5, 1, 2, 4, or 6 h. After the indicated time, cells were lysed and the proteins were collected. A, The activation of NF-κB was detected by EMSA. B, The phosphorylation of I-κB was assayed by Western blotting. The experiments were repeated twice.

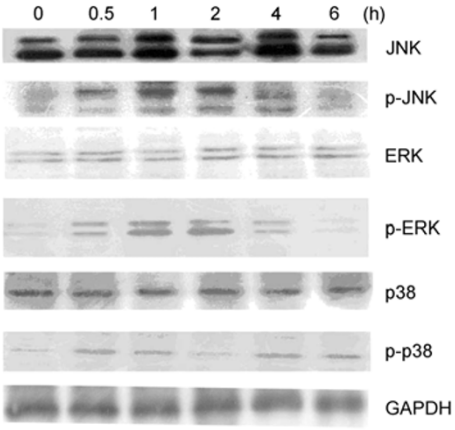

Figure 4 H_2O_2 induced the phosphorylation of MAPKs in RAW 264.7 macrophages. Cells were treated with 500 μmol L^{-1} hydrogen peroxide for either 0.5, 1, 2, 4, or 6 h. After the indicated time, cells were lysed and the proteins were collected. The phosphorylation of MAPKs including JNK, ERK and p38 was examined by Western blotting. These experiments were repeated at least twice.

the mechanism of the necrosis-to-apoptosis switch in H_2O_2 treated macrophages. As shown in Figure 6A, apoptosis is provoked by p38 and JNK. For necrosis, however, only JNK contributes to its activation. p38 is supposed to ensure the apoptosis transition from necrosis to apoptosis and JNK functions in the reverse direction. NF-κB and ERK repress both processes. The simulation results are shown in Figure 6B. Resembling Figure 2A, a necrosis-to-apoptosis switch appears around 4 h, indicating the precision of the models.

3 Discussion

In the present study, we detected cell death events in RAW

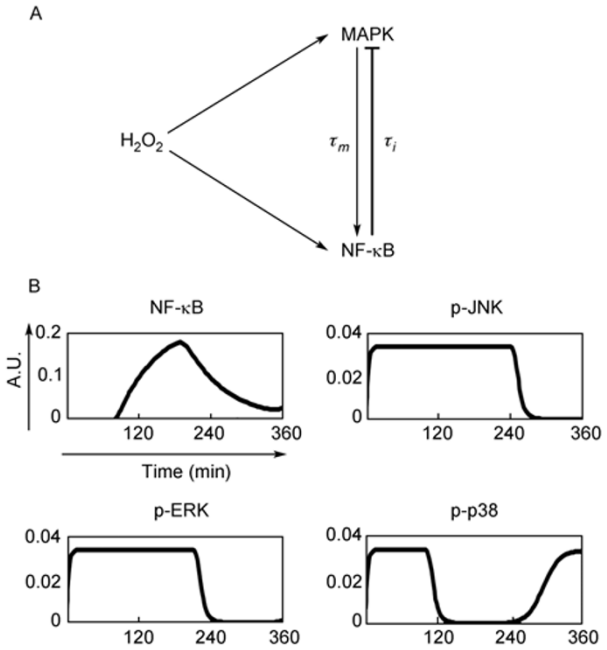

Figure 5 Predicting connections between NF-κB and MAPK via mathematical modeling. A, A simple model comprising MAPKs and NF-κB has been employed to capture the characteristics of their regulations. MAPKs and NF-κB are both activated by H_2O_2 treatment. MAPKs positively regulate NF-κB while they are repressed by NF-κB via negative feedback. τ_m and τ_i (i=1, 2, 3) respectively represent time delays of MAPKs dependent activation of NF-κB and NF-κB dependent inhibition of MAPKs. B, The simulating results resemble the activation patterns of NF-κB and MAPKs in Figures 3 and 4 (A.U.=arbitrary unit).

264.7 macrophages triggered by H_2O_2. We found that both apoptosis and necrosis coexisted, as seen in Figure 1A. As the consequence of apoptosis is recognized to be superior to that of necrosis for an entire organism, we did time-sequential measurements to determine whether a cell-death-mode switch between apoptosis and necrosis existed. Our results showed that the ratio of apoptotic cells to necrotic cells strongly went up after 4 h of treatment (Figure 2B). A number of intermediate cells undergoing necrosis-to-apoptosis change were observed via immunofluorescence (Figures 2C and E). We thus confirmed that the necrosis-to-apoptosis switch did occur in H_2O_2 treated RAW 264.7 macrophages.

The mechanisms underlying the cell death mode switch have been analyzed in several cell types, and a few conclusions have been proposed, including decreases in the intracellular level of ATP [15], inactivation of caspases [16], and regulation of Protein Kinase C [4]. However, never previously have NF-κB and MAPKs been mentioned to be involved in the switch mechanisms. Our data demonstrated the transient activation of NF-κB, JNK and ERK as well as re-activation of p38 around 4 h of treatment time (Figures 3 and 4). Therefore, we supposed that both NF-κB and MAPKs were critical factors in this cell-death-mode switch.

It has been reported that complicated connections exist

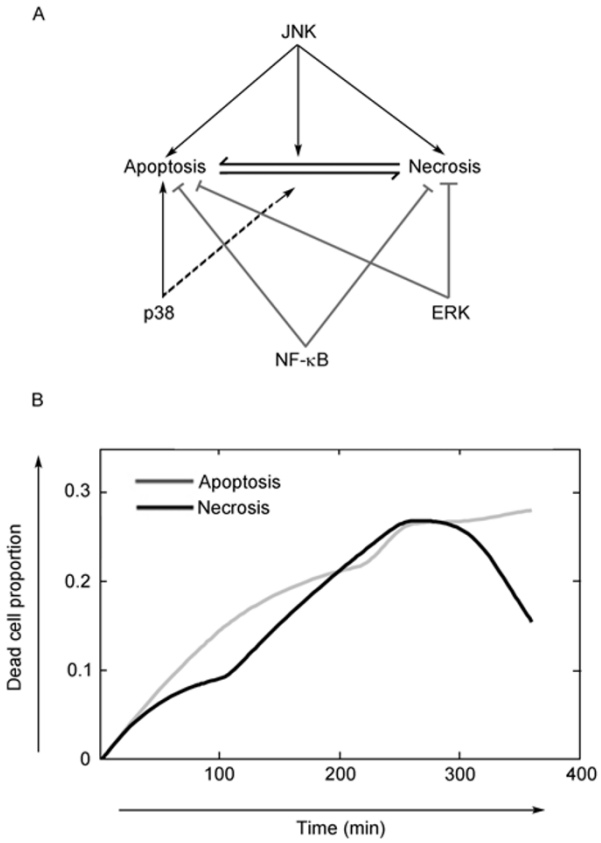

Figure 6 Simulating necrosis-to-apoptosis switch via mathematical modeling. A, A model including MAPKs and NF-κB is introduced to elucidate the mechanism of this cell-death-mode switch. Apoptosis is activated by p38 and JNK. For necrosis, however, only JNK contributes to its activation. Meanwhile, p38 is thought to ensure the apoptosis transition from necrosis to apoptosis and JNK functions in the reverse direction. NF-κB and ERK repress both processes. B, The simulating result resembles the cell-death-mode switch in Figure 1B.

between NF-κB and MAPKs. MAPKs are considered to be one kind of key inducer of NF-κB. Maritza Jaramillo *et al.* [12] found that ERK1/2 induced NF-κB activation in H_2O_2 treated macrophages. Eirini Kefaloyianni *et al.* [17] showed that both ERK and p38 were involved in NF-κB activation during oxidative stress. In addition, Vladimir S. Spiegelman reported that JNK activates NF-κB through the induction of β-TrCP [18]. While activated, NF-κB promotes the expression of several proteins which are inhibitors of MAPKs. For example, JNK is inhibited by NF-κB activation through up-regulation of the inhibitory proteins of JNK including GADD45β, XIAP, and c-FLIPL [19,20].

In accordance with these pieces of evidence and our data, we introduced a minimal mathematical model of NF-κB and MAPKs (respectively p-p38, p-ERK, p-JNK) interactions. As shown in Figure 5A, under oxidative stress, NF-κB and MAPKs become activated. Once activated, MAPKs positively regulated NF-κB activation with a time delay τ_m. Activated NF-κB inhibits upstream MAPK with distinct time delays (τ_i). Short delays indicate fast negative regulatory effects, while long delays denote slow negative regulations.

As shown in Figure 5B (τ_1=10 min), NF-κB is activated and elicits one pulse. NF-κB decreases p-p38 activation through a fast negative feedback loop. The activated level of MAPK declines at about 2 h. Note that p-p38 positively regulates NF-κB activation. As activated p-p38 reverts to a low level, NF-κB is deactivated. Deactivation of NF-κB increases the activation rate for p-p38 and hence induces a second p-p38 pulse at about 260 min. Upon increasing τ_i (e.g., τ_2=120 min), inhibition of p-ERK by NF-κB becomes a slow negative feedback loop, and as demonstrated above, the level of activated p-ERK drops owing to the NF-κB inhibitory effect. The time by which p-ERK reverts to the original steady state is at about 240 min showing a considerable delay about 120 min compared with a fast negative feedback. It shows one p-ERK pulse within 6 h. As τ_i further increases (τ_i=150 min), the time by which the levels of phosphorylated MAPK (p-JNK) decline is at about 290 min, which indicates a larger delay compared with p-ERK.

Based on the simulation results of the model mentioned above, we set out to investigate the regulatory mechanism of the necrosis-to-apoptosis switch mediated by NF-κB and MAPKs. NF-κB and ERK are believed to provide an anti-apoptotic function in macrophages, JNK is reported to aggravate macrophage necrosis and p38 is recognized to promote macrophage apoptosis [21–24]. Hence, we proposed a second model to illustrate MAPKs and NF-κB mediated apoptosis/necrosis regulatory effects. As shown in Figure 6A, apoptosis is activated by p38 and JNK. For necrosis, however, only JNK contributes to its activation. p38 is believed to ensure an apoptosis transition from necrosis to apoptosis and JNK functions in the reverse directions. NF-κB and ERK repress both processes. Resembling Figure 2A, apoptotic cells increase within 6 h (Figure 6B). Necrotic cells continue growing until about 4 h when their number decreases. At early times (probably within 4 h), the apoptosis (p38) and necrosis (JNK) promoting effects surpass the inhibitory effects, such that both the necrotic and apoptotic fractions keep growing. JNK and p38 induced conversion counteracts each other. 4 h later, levels of JNK and ERK decline with p38 contributing now and promoting the apoptosis transition from necrosis which represents the necrosis decrease. Simulation results show that bifurcation of apoptosis and necrosis may be ascribed to the temporal control by differential MAPK regulatory effects.

Taken together, a fast negative feedback loop (i.e., the inhibitory effect of NF-κB) ensures two MAPK (p-p38) pulses, while a fast loop only elicits one MAPK pulse (p-ERK and p-JNK) within 6 h. Simulation results show that although NF-κB negatively regulates MAPK activities, the diverse MAPK dynamical patterns are attributed to either fast or slow feedback loops (i.e., the time delays of τ_i). Further simulation results verified these two models.

Thoroughly analyzed mechanisms of cell-death-mode switches contribute to therapeutics. In our present study, it seems that the death mode of macrophages challenged with ROS may be switched. ROS is abundantly generated by innate immune cells to antagonize pathogen invasion, but ROS also does great harm to immune cells themselves, including mortality. The necrosis-to-apoptosis switch in macrophages under oxidative stress restrains the number of necrotic cells, protecting the entire organism from excessive inflammation. Herein, the simulation results demonstrate that this switch may be mediated by the regulations of MAPKs and NF-κB, providing significant data for use in subsequent investigations.

We thank Mr. Owen Young of the University of Rochester School of Medicine and Dentistry for critical comments and editorial assistance. This work was supported by the National Natural Science Foundation of China (*Grant No. 30870588*)*, the Science Fund for Creative Research Groups* (*Grant No. 30821006*) *and the Program for New Century Excellent Talents in University* (*Grant No. NCET-06-0445*)*.*

1 Marcin K, Edyta N, Makoto M, *et al.* The switch mechanism of the cell death mode from apoptosis to necrosis in menadione-treated human osteosarcoma cell line 143B cells. Microsc Res Techniq, 2004, 64: 255–268
2 Susan L F, Brad T C. Apoptosis, pyroptosis, and necrosis: mechanistic description of dead and dying eukaryotic cells. Infect Immun, 2005, 73: 1907–1916
3 Naoyuki S, Koichi I. Nicotine switches the form of H_2O_2-induced cell death from apoptosis to necrosis in U937 cells. Immunol Lett, 2000, 72: 163–166
4 Kim C H, Han S I, Lee S Y, *et al.* Protein kinase C-ERK1/2 signal pathway switches glucose depletion-induced necrosis to apoptosis by regulating superoxide dismutases and suppressing reactive oxygen species production in A549 lung cancer cells. J Cell Physiol, 2007, 211: 371–385
5 Diane M S, Joyce A B. Cyclic AMP differentiation of the oligodendroglial cell line N20.1 switches staurosporine-induced cell death from necrosis to apoptosis. J Neurosci Res, 2001, 66: 691–697
6 Liu H, Ma Y, Pagliari L J, *et al.* TNF-α-induced apoptosis of macrophages following inhibition of NF-κB: a central role for disruption of mitochondria. J Immunol, 2004, 172: 1907–1915
7 Chen Y, Smith M R, Thirumalai K, *et al.* A bacterial invasion induces macrophage apoptosis by binding directly to ICE. Embo J, 1996, 15: 3853–3860
8 Tracie D S, Yankun L, Pin M Y, *et al.* Cholesterol-induced macrophage apoptosis requires ER stress pathways and engagement of the type A scavenger receptor. J Cell Biol, 2005, 171: 61–73
9 Shen H M, Zhang Z, Zhang Q F, *et al.* Reactive oxygen species and caspase activation mediate silica-induced apoptosis in alveolar macrophages. Am J Physiol Lung Cell Mol Physiol, 2001, 280: 10
10 Sawyer R T, Dobis D R, Goldstein M, *et al.* Beryllium-stimulated reactive oxygen species and macrophage apoptosis. Free Radic Biol Med, 2005, 38: 928–37
11 Takuya N, Ken I, Hisashi F, *et al.* Requirement of reactive oxygen species-dependent activation of ASK1-p38 MAPK pathway for extracellular ATP-induced apoptosis in macrophage. J Biol Chem, 2008, 283: 7657–7665
12 Maritza J, Martin O. Hydrogen peroxide induces murine macrophage chemokine gene transcription via extracellular signal-regulated kinase- and cyclic adenosine 5′-monophosphate (cAMP)-dependent pathways: involvement of NF-κB, activator protein 1, and cAMP response element binding protein. J Immunol, 2002, 169: 7026–7038
13 Tarek B, Eric C, Peter M. Mitogen-activated protein (MAP) kinase/MAP kinase phosphatase regulation: roles in cell growth, death, and cancer. Pharmacol Rev, 2008, 60: 261–310
14 Dutta J, Fan Y, Gupta N, *et al.* Current insights into the regulation of programmed cell death by NF-κB. Oncogene, 2006, 25: 6800–6816
15 Marcel L, Barbara S, Anna F C, *et al.* Intracellular adenosine triphosphate (ATP) concentration: a switch in the decision between apoptosis and necrosis. J Exp Med, 1997, 185: 1481–1486
16 Marek L, Malgorzata M, Davide F, *et al.* Activation and caspase-mediated inhibition of PARP: a molecular switch between fibroblast necrosis and apoptosis in death receptor signaling. Mol Biol Cell, 2002, 13: 978–988
17 Eirini K, Catherine G, Isidoros B, *et al.* ERK1/2 and p38-MAPK signalling pathways, through MSK1, are involved in NF-κB transactivation during oxidative stress in skeletal myoblasts. Cell Signal, 2006, 18: 2238–2251
18 Vladimir S S, Pete S, Esther L, *et al.* Induction of β-transducin repeat-containing protein by JNK signaling and its role in the activation of NF-κB. J Biol Chem, 2001, 276: 27152–27158
19 Zhang Y, Chen F. Reactive oxygen species (ROS), troublemakers between nuclear factor-κB (NF-κB) and c-Jun NH2-terminal kinase (JNK). Cancer Res, 2004, 64: 1902–1905
20 Akihito N, Sachiko K, Mutsuhiro T, *et al.* An antiapoptotic protein, c-FLIPL, directly binds to MKK7 and inhibits the JNK pathway. EMBO J, 2006, 25: 5549–5559
21 Jin M P, Florian R G, Athena W, *et al.* Signaling pathways and genes that inhibit pathogen-induced macrophage apoptosis—CREB and NF-κB as key regulators. Immunity, 2005, 23: 319–329
22 Manikandan S, Chandrima S. Up-regulation of Bcl-2 through ERK phosphorylation is associated with human macrophage survival in an estrogen microenvironment. J Immunol, 2007, 179: 2330–2338
23 Ventura J J, Cogswell P, Flavell R A, *et al.* JNK potentiates TNF-stimulated necrosis by increasing the production of cytotoxic reactive oxygen species. Genes Dev, 2004, 18: 2905–2915
24 Iwaoka S, Nakamura T, Takano S, *et al.* Cationic liposomes induce apoptosis through p38 MAP kinase-caspase-8-Bid pathway in macrophage-like RAW264.7 cells. J Leukoc Biol, 2006, 79: 184–191